IOP Conf. Series: Materials Science and Engineering **117** (2016) 012035 doi:10.1088/1757-899X/117/1/012035

Effect of Ce melt treatment on solidification path of ZA8 alloy

R Sudheer, V Vijeesh and K N Prabhu[a]
Department of Metallurgical & Materials Engineering, National Institute of Technology Karnataka, Surathkal, Mangalore 575 025, India

E-mail: [a]prabhukn_2002@yahoo.com

Abstract. The solidification path of ZA8 alloy with Ce addition was characterized using Newtonian technique of thermal analysis. The solidification events were determined using cooling curve and its first derivative curve. The microstructure and chemical composition of various phases in the alloy were studied using EDS, SEM and XRD techniques. It was found that the addition of Ce did not cause formation of new phases. However, it hinders the nucleation of stable β dendrites in the alloy. The presence of Ce promotes the eutectoid phase transformation and increases the hardness of the alloy. Latent heat of solidification and heat of eutectoid transformation were found to increase on Ce addition. The upward solidification of the alloy against Cu chill was analysed. Chilling had significant influence on solidification parameters, and caused refinement of the microstructure. The addition of Ce to the melt had no effect during chill casting of the alloy.

1. Introduction

Zinc–Aluminium base alloys are used for many industrial applications by virtue of their excellent physical and mechanical properties such as good machinability, high as-cast strength, excellent bearing properties, corrosion resistance, fine surface finish, ability to cast thin sections, as well as low energy requirements (for melting). Among ZA alloys only ZA8 can be hot chamber die cast due to its low melting point. This reduces the production cost of ZA8 for industrial purpose compared to that of other ZA alloys [1,2]. The mechanical properties of ZA alloys mainly depend on the presence and amount of various impurities, and the final microstructure of casting [2].

The effect of melt treatment on the cooling curve, microstructure and various mechanical properties of the alloy is discussed by various researchers. Turk et al. studied the effect of addition of Mn on the microstructure and mechanical properties of ZA8 alloy. The addition of Mn modifies the as cast microstructure by refining the β dendrites and increasing the amount of eutectic phase, and also forms a fine and irregularly shaped intermetallic compound (MnAl6). The hardness and creep strength of the ZA8 alloy increased with manganese content, whereas 0.2% yield, tensile and impact strengths of the alloy improved with increasing Mn up to 0.045 wt-% and then reduced with a further increase in manganese. [1]. Turk et al. reported that ZA-8 alloy when modified with Pb, Sn and Cd resulted in higher wear resistance. Metallographic studies showed that the addition of Pb, Sn and Cd resulted in modification of the microstructure of ZA8 alloy [3].

Ramesh et al. studied the effect of Mn addition to ZA8 alloy on thermal analysis parameters, heat transfer and microstructure. The addition of Mn to ZA8 alloy increased the contact angle, indicating decreased wettability of the modified alloy on the chill surface. The microstructure of ZA8 with Mn showed an increased amount of β phase and a decreased amount of eutectic [2]. Ramesh and Prabhu found that the chill material and coating had a significant effect on the cooling curve of ZA8 alloy. It

IOP Conf. Series: Materials Science and Engineering **117** (2016) 012035 doi:10.1088/1757-899X/117/1/012035

was found that chilling during solidification causes the morphology of dendrites transform to nearly rounded shape with refinement of lamellar eutectic [4,5].

Zhu et al. observed that the Cu modified ZA8 alloy consists of a tree stem shaped eutectic structure together with flower-like cores of solidification, which were surrounded by a large amount of eutectoid structure. Further ageing at 150°C results in decomposition of zinc rich η phase and four-phase transformation, $\alpha+\varepsilon\rightarrow T'+\eta$ [6].

Krupinska et al. reported that the increase in cooling rate results in refinement of the microstructure as well as increase in the alloy hardness. They found that the addition of La and Ce into ZnAl8Cu1 alloy causes only refinement of grains and sub grains in the microstructure but no occurrence of new phases or eutectics during solidification of the alloy [7].

Thermal analysis is a useful tool for the non-destructive assessment of melt quality. The Newtonian and Fourier techniques have been successfully used to calculate latent heat and solid fraction distribution using cooling curve analysis [8]. Haq et al. have shown that to obtain the baseline for calculating the latent heat, polynomial and exponential fitting methods show inaccuracy and inconsistency in the obtained results. On the other hand, the results obtained by fitting the first derivative curve (FDC) linearly are reproducible [9].

Among ZA alloys which are known for superior hardness, wear strength and other mechanical properties, ZA8 alloy has found limited industrial applications. Melt treatment of ZA8 alloy with Ce to modify microstructure and improve mechanical properties can prove to be beneficial. Though thermal analysis of various Al alloys have been done in the past, the solidification path of ZA8 alloy has not been characterized. The data obtained from thermal analysis would be useful for melt quality control in foundries.

2. Experimental

The nominal composition of ZA8 alloy is given in Table 1. ZA8 samples of about 800g were heated in a clay-graphite crucible up to 480°C, and Ce ingots (Alfa-Aesar, USA) were then added to prepared samples having varying Ce compositions of 0.25%, 0.5% and, 1.0% by weight. The furnace holding time was 30 minutes.

Table 1. Composition of ZA8 alloy.

Elements	Al	Cu	Mg	Fe	Sn	Cd	Pb	Ni	Zn
Wt-%	8.2-8.8	0.8-1.3	0.02-0.03	0.065	0.005	0.005	0.005	…	Balance

Calibrated K-type thermocouples (0.45ϕ) enclosed in twin bore ceramic beads were used as temperature sensors. A scanning frequency of 10Hz was selected during the temperature data acquisition. A Data Acquisition System (NI USB 9162) was used for this purpose. The temperature data acquired from thermal analysis was later processed and analyzed to obtain cooling curves and first derivatives of cooling curves (FDC).

Samples were tested in X-ray diffractometer (JEOL JDX-8P-XRD) to obtain XRD patterns. Polished samples were etched with 10% HF. JEOL Analytical SEM (JSM 6380LA) and ZEISS optical microscope (AXIOIMAGER) were used for microstructure examination. Energy Dispersive Spectroscopy (EDS) analysis was also carried out. For hardness testing, samples of ZA8 alloy having 0.05m thickness and 0.05m diameter were prepared and tested as per the ASTM E10 standards. The Brinell Hardness Number (BHN) was measured at 500kg load with a steel ball indenter of 10mm diameter. Cu chills of length 0.05m and diameter of 0.05m were prepared to study the influence of high cooling rates on upward solidification of ZA8 alloy.

3. Results and discussion

Figure 1 shows the cooling curve of ZA8 alloy. Crystals of Zn rich β phase nucleate as the alloy cools below the liquidus temperature. The occurrence of Zn rich eutectic η is observed at the eutectic arrest temperature and, the simultaneous growth of these two phases arrest the cooling curve at the eutectic temperature until the whole liquid alloy gets solidified. Later, at eutectoid temperature, the β phase transforms into eutectic η and Al rich α phase.

From the cooling curve analysis the liquidus, solidus and eutectoid transformation temperatures were found to be 406.7°C, 375.5°C and 252.5°C respectively for ZA8 alloy. The addition of Ce resulted in a drop in the liquidus temperature with undercooling while, the other parameters remained unchanged**.** The magnified region around the liquidus temperature is shown in figure 2. Table 2 gives the effect of Ce addition on liquidus temperature during solidification of ZA8.

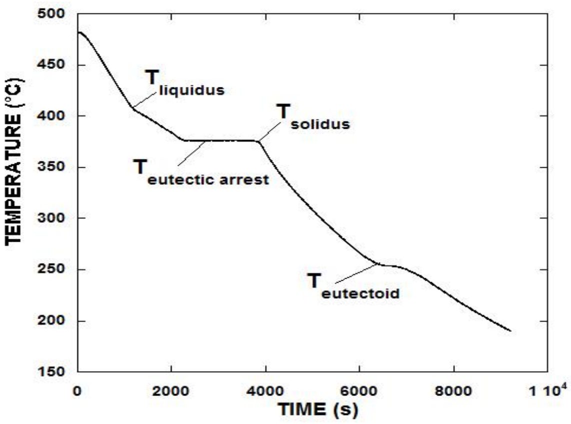

Figure 1. Cooling curve of ZA8 alloy.

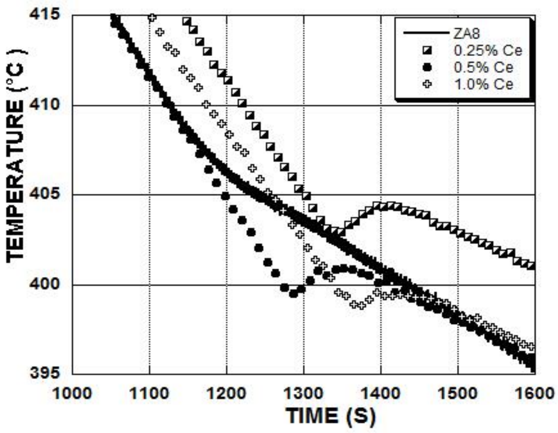

Figure 2. Effect of Ce on liquidus temperature.

Table 2. Effect of Ce addition on Liquidus Temperature during solidification of alloy.

	Liquidus Temperature (˚C)					Undercooling (˚C)
	Trial 1	Trial 2	Trial 3	Mean	Std. Deviation	
ZA8	406.6	406.7	406.9	406.7	0.152	-
ZA8+ 0.25% Ce	404.7	403.8	403.7	404.0	0.550	2.0
ZA8+ 0.50% Ce	401.5	399.6	400.9	400.6	0.971	2.0
ZA8+ 1.0% Ce	398.6	400.3	399.7	399.5	0.862	1.0

In figure 3, the cooling rate curve of ZA8 alloy shows a small valley between point **a** and point **b**. The presence of peaks **a'** and **a''** are attributed to the melting and solidification of unstable β phase dendrites. On addition of Ce, the peak **a'** became more pronounced in the same region. It clearly confirms that Ce hinders the nucleation of stable β dendrites. The peak at the liquidus point **a**, was attributed to the liquidus undercooling on addition of Ce.

The binary phase diagram of Al-Ce and Zn-Ce system show that Ce has almost zero solubility in Al and Zn at the melt treatment temperature of 480°C. Ce has a higher atomic radius compared to Zn and Al and its accumulation around the nucleation sites must hinder the diffusion of Zn atoms in the melt which in turn decreased the nucleation rate of β dendrites. As solidification progressed, the increase in concentration of Ce in the melt further decreases the rate of formation of stable β phase. This was observed as a more pronounced peak in the cooling rate curves.

IOP Conf. Series: Materials Science and Engineering **117** (2016) 012035 doi:10.1088/1757-899X/117/1/012035

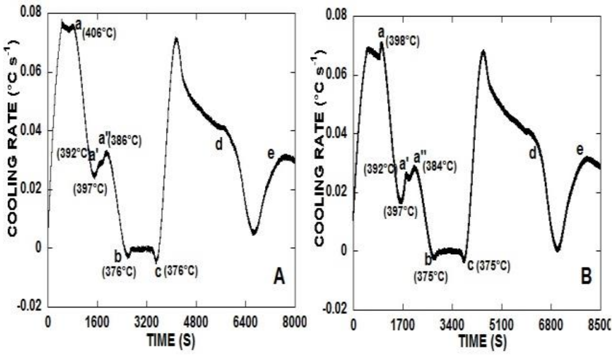

Figure 3. Cooling rate curve, (A) ZA8, (B) ZA8+1.0%Ce.

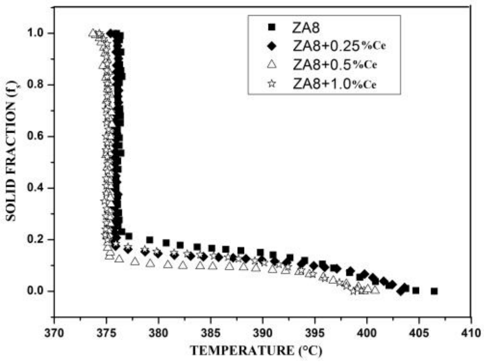

Figure 4. Effect of Ce on Solid Fraction curves.

The Newtonian technique of computer aided cooling curve analysis was used to quantify the effect of Ce addition on latent heat of solidification and the heat of eutectoid transformation. In the first derivative curve (FDC), the start and end points of solidification and eutectoid transformation were fitted linearly to obtain the baseline. The difference between the area under the FDC and the baseline, when multiplied with specific heat capacity (C_p) of the alloy yields the latent heat evolved and the heat of eutectoid transformation. The C_p value of alloy was taken as 435J/kg.K [10]. Table 3 shows that the addition of Ce increases the latent heat evolved and the heat of eutectoid transformation. Increase in latent heat is reflected in the cooling curve as a slight increase in the solidification time on addition of Ce. The significant increase in the heat of eutectoid transformation on addition of Ce shows that Ce promotes eutectoid transformation in the alloy.

Table 3. Effect of Ce addition of heat of phase transformation.

Specimen composition	ZA8	ZA8+0.25%Ce	ZA8+0.5%Ce	ZA8+1.0%Ce
Latent heat (kJ/kg)	55.68	59.85	60.55	60.90
Heat of eutectoid transformation (kJ/kg)	11.20	12.30	12.43	13.04

In figure 4, solid fraction (f_s) curves corresponding to alloys with Ce, lags behind that of ZA8 alloy during nucleation and growth of β phase. This confirms the fact that Ce hinders the formation of stable β dendrites. The f_s values at the eutectic arrest temperature decreased on addition of Ce. Thus, it is evident that the η to β ratio at the end of fusion should be high on addition of Ce. The increase in latent heat of fusion can be attributed to this effect. The XRD pattern of casting samples showed no additional peaks. It indicates that melt treatment did not cause occurrence of any new phase or eutectics during solidification of the alloy.

Figure 5 shows the effect of Ce addition on microstructure of ZA8 alloy. Addition of Ce influenced the morphology of retained β dendrites. A significant decrease in the size and distribution of β, and an increase in the volume fraction of eutectic η were observed on addition of Ce. Ce promotes the disintegration of β dendrites into eutectic η and the Al rich α phase. The mechanism of eutectoid transformation is not well understood.

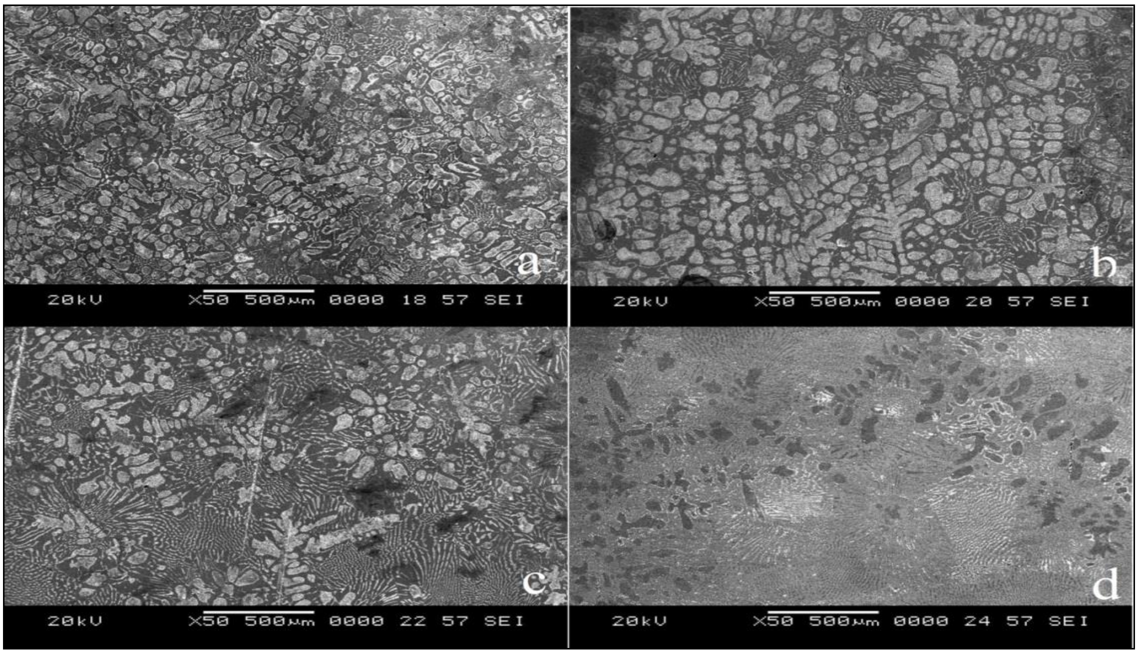

Figure 5. Microstructure (a) ZA8, (b) ZA8+0.25% Ce, (c) ZA8+0.5% Ce, (d) ZA8+1.0% Ce.

EDS analysis of the casting samples were carried out. The presence of Ce was detected only in β phase and eutectic η while, it remained absent in α phase, as shown in figure 6. Further, Ce was detected only in the outer shell of the β dendrite due to intergranular segregation of Ce. After eutectoid transformation, the Ce atoms, dispersed in the newly formed α phase, diffuses into the retained β phase and newly formed eutectic η.

The effect of chilling on solidification parameters and microstructure was investigated using Cu chills. The solidification range of ZA8 alloy reduced to 9°C between 410°C and 401°C on chilling, as shown in figure 7. The eutectoid transformation was observed at around 343°C. The nucleation rate being very high on chilling, the role of Ce in hindering the formation of stable β phase was found to be insignificant.

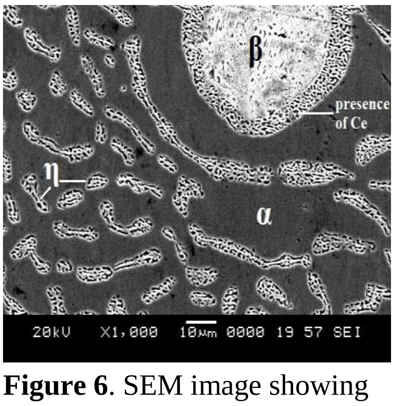

Figure 6. SEM image showing the accumulation of Ce at outer shell of β dendrite

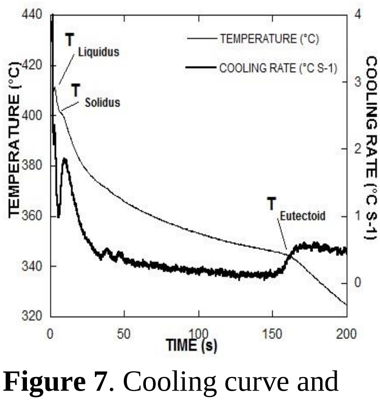

Figure 7. Cooling curve and Cooling rate curve on chilling

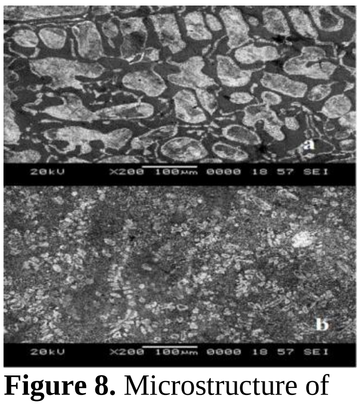

Figure 8. Microstructure of ZA8 (a) crucible cooled (b) chill cast

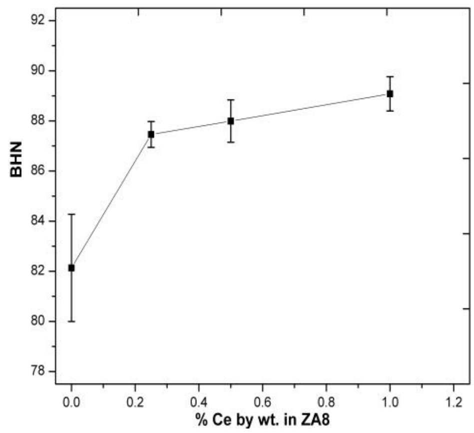

Figure 9. Effect of Ce on BHN of ZA8

The microstructure study of the chilled ZA8 sample showed very fine structure of β phase and eutectic η, as shown in figure 8. Addition of Ce had no effect on the microstructural evolution of the chilled samples. Unlike furnace cooled cast samples, the chilled alloy samples show the presence of Ce in the α phase. Complete diffusion of Ce atoms from the α phase back into the retained β and into the newly formed eutectic η could not occur due to high cooling rates. The addition of Ce had an effect on hardness of ZA8 alloy. Brinell hardness of graphite crucible cooled ZA8 sample was observed to increase with increase in Ce content as shown in figure 9. This change was due to the increase in volume fraction of fine eutectic η particles.

From the phase diagram of Zn-Al system, we can predict that on equilibrium cooling rates, complete transformation of β phase into α phase and very fine eutectic η can be obtained without addition of Ce. The refined microstructure can also be attained at high cooling rates. Though the microstructure obtained is refined in both the cases, the constituent phases are different. The former offers well dispersed η phase grains in the α phase matrix while, the latter contains retained β phase dendrites as well. Addition of Ce offers well dispersed β phase and eutectic η in the α phase matrix even at moderate cooling rates.

4. Conclusions

- The melt treatment of ZA8 alloy with Ce hinders the nucleation of stable β phase. A drop in liquidus temperature and additional peaks in the cooling rate curve indicate the presence of unstable β phase.
- The addition of Ce promotes eutectoid phase transformation in ZA8 alloy. The refined microstructure of ZA8 alloy with Ce addition showed an increase in the volume fraction of η-phase.
- Latent heat of solidification and the heat of eutectoid transformation increased on addition of Ce.
- The addition of Ce increases the hardness of the as cast ZA8 alloy.
- Chilling had a significant effect on the solidification parameters, and caused the refinement of microstructure of ZA8 alloy. Addition of Ce had no significant influence on solidification and microstructure of chill cast ZA8 alloy.

References

[1] Turk A, Durman M, and Kayali E S 2007 *J. Mater. Sci*. **42** 8298.
[2] Ramesh G, Vishwanath H M, and Prabhu K N 2012 Mater. Sci. Technol. 28(11) 1301.
[3] Turk A, Kurnaz C, and Sevik H 2006 Mater. Design. 28 1889.
[4] Ramesh G, and Prabhu K N 2012 *Inter. J. Cast Met. Res*. **25**(3) 160.
[5] Ramesh G, and Prabhu K N 2012 *Trans. Indian. Inst. Met*. **65**(6) 719.

IOP Conf. Series: Materials Science and Engineering **117** (2016) 012035 doi:10.1088/1757-899X/117/1/012035

[6] Zhu Y H, Lee W B, To S 2003 *J. Mater. Sci.* **38** 1945.
[7] Krupińska B, Rdzawski Z, and Labisz K 2011 *J. Achievements Mater. Manuf. Eng.* **46** (2) 154.
[8] Djurdjevic M B, Odanovic Z, and Talijan N 2011 *J. Minerals Met. Mater. Soc.* **30**(11) 51.
[9] Haq I, Shin J, and Lee Z 2004 *Met. Mater. Int.* **10**(1) 89.
[10] Alloy data 2006 NADCA Product Specification Standards for Die Castings A-3-14-06.